Theor Chem Acc (2000) 104:203–206
DOI 10.1007/s002140000144

Theoretical
Chemistry Accounts

Regular article

$\tilde{X}^2A'/\tilde{A}^2A'$ conical intersection effects on the fluorescence of NO_2

Fabrizio Santoro

Dipartimento di Chimica, Università di Siena, Via Aldo Moro, 53100 Siena, Italy
e-mail: fabrizio@hare.icqem.pi.cnr.it

Received: 16 September 1999 / Accepted: 3 February 2000 / Published online: 5 June 2000

Abstract. We have analyzed the effect of the $\tilde{X}^2A'/\tilde{A}^2A'$ conical intersection between the first two electronic surfaces of NO_2 on the fluorescence of the molecule. Our computations are based on diabatic potentials obtained by a transformation of ab initio adiabatic potentials. We have computed time- and frequency-resolved fluorescence spectra from stationary and nonstationary states, showing the effects of the conical intersection, which slows down the fluorescence, shifts the emitted frequencies, redistributes the intensities, and increases the density of the lines. Furthermore, we have explained the low fluorescence yield observed by Dulcey et al. after optical excitation.

Key words: Conical intersection – Nonadiabatic effects – Time- and frequency-resolved fluorescence

1 Introduction

The Born–Oppenheimer (BO) adiabatic approximation is a cornerstone in chemical physics. It neglects the effects of the nuclear kinetic energy on the electronic motion since these give rise to nonadiabatic couplings between different BO electronic states which are usually very weak compared to their energy difference [1]. This approximation completely breaks down on the occurrence of degenerations between adiabatic potentials because the nonadiabatic couplings diverge along the intersection loci [1], generally referred to as conical intersections. These are a common feature in polyatomic molecules and can rule their internal dynamics and optical behavior [1–3].

The NO_2 molecule is one of the best examples where such nonadiabatic effects have been predicted theoretically and observed experimentally. In fact, the conical intersection between the first two adiabatic potentials, $\tilde{X}^2A'$ and $\tilde{A}^2A'$, gives rise to very complex spectra and internal dynamics [4–18]. In our previous work we investigated the effects of the conical intersection on the absorption spectrum, the internal dynamics, and the radiative lifetimes of NO_2. Here we extend our analysis to the time- and frequency-resolved spectra of stationary and nonstationary states of the molecule, suggesting an explanation for the low fluorescence yield observed by Dulcey et al. [19] after excitation at 18794 cm^{-1}, in the range of the emitted photon energy from excitation to 15239 cm^{-1}.

2 Time- and frequency-resolved probability of spontaneous emission of a photon

The decay rate of an eigenstate $|n\rangle$ due to spontaneous emission is obtained by summing the emission rates over all the possible final states $|n\rangle$ with energies $E_{n'} < E_n$

$$\gamma_n = \sum_{n'} \gamma_{n'n} = \sum_{n'} \frac{4\omega_{nn'}^3}{3\hbar c^3} |\langle n|\mathbf{d}|n'\rangle|^2 \ , \tag{1}$$

where $\omega_{nn'} = (E_n - E_{n'})/\hbar$ and $\mathbf{d}$ is the electric dipole of the molecule. The radiative lifetime of the state $|n\rangle$ is $\tau_n = 1/\gamma_n$.

The time- and frequency-resolved probability density for emitting a photon from a molecular eigenstate $|n\rangle$ is equal to [20]

$$\frac{dP_n(\omega,t)}{d\hbar\omega} = \frac{2\omega}{3\pi\hbar^2c^3} \sum_{n'} [1 + \exp(-\gamma_n t) - 2\exp(-\gamma_n t/2) \cos(\omega_{nn'} - \omega)t] \frac{|\langle n|\mathbf{d}|n'\rangle|^2 \omega_{nn'}^2}{(\omega_{nn'} - \omega)^2 + \gamma_n^2/4} \ , \tag{2}$$

which represents a series of bands centered at the resonance frequencies $\omega_{nn'}$, with a width depending on $\gamma_{nn'}$, each corresponding to transitions toward the $|n'\rangle$ state. In the case of NO_2, at time long enough (tens of picoseconds) and because of the sharpness of the bands ($\gamma_{nn'} \approx 10^{-7} cm^{-1}$, the emission probability is better represented as a series of lines with heights equal to the areas under the corresponding bands of Eq. (2),

$$P_n(\omega,t) = \begin{cases} (\gamma_{nn'}/\gamma_n)[1 - \exp(-\gamma_n t)] & \omega = \omega_{nn'} \quad \forall\, n' \\ 0 & \omega \neq \omega_{nn'} \quad \forall\, n' \end{cases} . \tag{3}$$

The computation is considerably more complicated if the molecule is initially excited in a nonstationary state and we have worked out a theoretical scheme to deal with this general case [20]; however, even in this case the computation is simplified if we limit our investigation to the long-time limit with respect to the times of the internal dynamics. The NO_2 intramolecular dynamics following the excitation is so fast and complex that the wave packet has undergone a complete dephasing in about 1 ps and the molecule then behaves as if it was prepared in a statistical mixture of states. Thus, in the long-time limit, the probability of emission from a nonstationary state $|I\rangle$ can be computed as a weighted average of the probability of emission from the individual molecular eigenstates with weights equal to the populations $|\langle n|I\rangle|^2$,

$$P_I(\omega,t) = \begin{cases} |\langle n|I\rangle|^2(\gamma_{nn'}/\gamma_n)[1-\exp(-\gamma_n t)] & \omega=\omega_{nn'} \quad \forall\, n,n' \\ 0 & \omega\neq\omega_{nn'} \quad \forall\, n,n' \end{cases} . \tag{4}$$

The accuracy of this approximation has been confirmed by numerical tests.

To conclude this section we note that, in the limits we are considering, the result of a photon-counting experiment between time t_1 and time t_2, after the excitation to a general state $|k\rangle$, is proportional to the quantity

$$S_k(\omega) = P_k(\omega,t_2) - P_k(\omega,t_1) \ . \tag{5}$$

Hereafter we always suppress the labels k, t_2, and t_1, it always being clear which are the initial state and the times under investigation.

3 Nonadiabatic states and Franck–Condon approximation

The NO_2 nonadiabatic states up to 18735 cm^{-1}, their energies, and their emission rates have been previously obtained in a diabatic electronic representation 1^2A_1 and 1^2B^2 [10,16,18]. The spectra are calculated in the Franck–Condon (FC) approximation for the dipole moment whose active component is of B_2 symmetry. We suppose that before optical excitation the NO_2 molecule is in the ground state of A_1 symmetry, which is very well approximated by the ground state vibrational species of 1^2A_1. Therefore the emitting species are of B_2 symmetry.

4 Results and discussion

4.1 Radiative quantum yield

The conical intersection $\tilde{X}^2A'/\tilde{A}^2A'$ strongly influences the fluorescence of the excited states of NO_2. Since 1954 it has been well known [21] that the radiative lifetimes of the NO_2 states are much longer than those expected on the basis of the integrated absorption coefficient. This feature is due to the nonadiabatic couplings which mix dark and bright states, slowing down the spontaneous emission of the latter states [18].

In 1980 Dulcey et al. [19] excited NO_2 at 18794 cm^{-1} and observed a collision-free fluorescence quantum yield of 16 ± 4% for $\hbar\omega$ 15239 cm^{-1}. They claimed that this yield is too low if one considers that the fluorescence is measured in the energy range more favored by the ω^3 factor, see Eqs. (1) and (3), and suggested two possible explanations: emission of lower-frequency photons and trapping of the excitation energy as internal energy.

As far as the second explanation is concerned, it should be noted that such energy trapping can occur only if the molecule is excited in a nonstationary state. This seems unlikely in the case under examination, since the width of the excitation pulse [19] was only 1.4 cm^{-1} (half width at half maximum) and NO_2 has one vibronic level per 7–8 cm^{-1} at about 18794 cm^{-1}, according to the experimental integrated density of levels [8].

Our results strongly suggest that the low quantum yield is due to emission of lower-frequency photons. Note that, because of the excitation energies and the detected range of emission, the authors measured fluorescence toward nonadiabatic states with energies below about 3500 cm^{-1}. For a level $|n\rangle$ let us consider

$$R_n = \sum_p \gamma_{pn} \Big/ \sum_q \gamma_{qn}, \quad \text{with } E_p < 3500\text{cm}^{-1} < E_n \quad \text{and} \quad E_q < E_n \ , \tag{6}$$

i.e. the ratio between the number of photons emitted by decaying into a state below 3500 cm^{-1} and the total number of emitted photons.

Since we computed the nonadiabatic states up to 18735 cm^{-1}, we cannot calculate R_n for the experimental initial level which is at higher energies. Anyway, the calculation of a NO_2 level at about 18800 cm^{-1} with an accuracy of about 1 cm^{-1} with respect to the experiment is beyond the present state of the art; therefore, any attempt to explain the experimental feature must be based only on the general trend of the results for computed levels close to the experimental one.

Thus, we divided the spectrum into adjacent windows with widths of 500 cm^{-1}, starting at 13250 cm^{-1}, and we computed the average $\langle R_n\rangle$ and its root-mean-square deviation in each window. The results are reported in Fig. 1, where each $\langle R_n\rangle$ is conventionally assigned to the average energy of the corresponding window. In the lower panel of Fig. 1 we have considered all the $|n\rangle$ states lying in the windows, while in the upper panel we have chosen only those whose absorption intensity is greater than 5% of the intensity of the strongest band in the window considered. The choice of the upper panel is due to the fact that in absence of more detailed information it could be supposed that the Dulcey et al. [19] excited a rather strong absorption band.

The trend of our results shows that at excitation energies comparable to the experimental one most of the photons are emitted in a frequency range lower than that investigated by Dulcey et al. [19]. To be more precise, our results suggest that at excitation energies of about 18500 cm^{-1} only 23 ± 14% of the photons are emitted in the frequency range they investigated, in good agreement with the experimental fluorescence yield of 16 ± 4%. By restricting our analysis to the strong

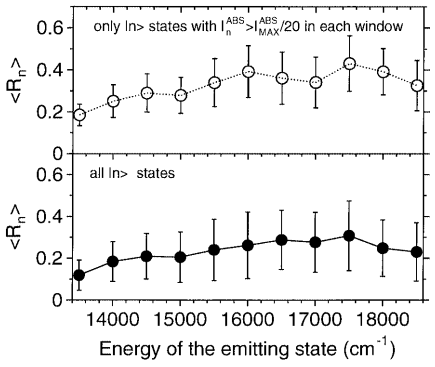

Fig. 1. $\langle R_n \rangle$ between the number of photons emitted in transitions toward final states at energies lower than 3500 cm^{-1} and the total number of emitted photons. *Lower panel*: for each window we consider all the computed states $|n\rangle$. *Upper panel*: for each window we consider only the $|n\rangle$ states with an absorption intensity greater than 5% of the intensity of the strongest band. See text for further details

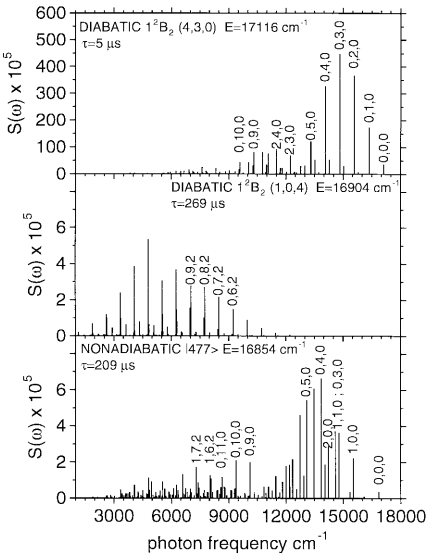

Fig. 2. Time- and frequency-resolved photon-counting spectra of stationary states computed in the time window from 150 to 300 ns

absorption bands (upper panel in Fig. 1) our estimate increases to 33 ± 12%, but it is still in semiquantitative agreement with the experimental measurements. These facts suggest that the observed low fluorescence quantum yield [19] is due to the strong emission of photons with energies lower than those investigated experimentally. The emission of low-frequency photons is caused by the shapes of the electronic potentials which, on one hand, lead to nonnegligible FC factors from the initial B_2 states to many A_1 final states and, on the other hand, lead to a large density of high-energy A_1 states, which compensates the effect of the ω^3 factor of Eq. (1), which favors transitions to low-lying A_1 states with emission of high-frequency photons.

4.2 Conical intersection effects on emission from a stationary state

The conical intersection $\tilde{X}^2A'/\tilde{A}^2A'$ strongly influences the fluorescence of the stationary states of the system, since it modifies both the initial stationary states in which the molecule is optically excited and the final stationary states in which the molecule decays after emission. This produces shifts in the frequencies of the emitted photons and redistribution of the intensities. To show these effects we chose an initial level and we computed the photon emission in a given time window, by neglecting (diabatic) or considering (nonadiabatic) the nonadiabatic couplings. We selected the 1^2B_2 (1, 0, 4)[1] diabatic state lying at 16904 cm^{-1} or the $|477\rangle$ nonadiabatic state at 16854 cm^{-1} (the 477th state in order of increasing energy) with the strongest contribution (21%) from (1,0,4) 1^2B_2 state. Note that the $|477\rangle$ weighting of the dark 1^2A_1 vibrational species is about 70% and that other zero-order 1^2B_2 states contribute to $|477\rangle$, for example, the (3, 0, 2) 2.6%, the (2, 2, 2) 1.7%, the (4, 3, 0) 1.1%, the (0,10,0) 0.5%, and the (6,0,0) 0.5%. The chosen initial state, in both the diabatic and nonadiabatic cases, is very weakly absorbing from the ground state because of the excited antisymmetric stretching and thus it cannot be prepared by optical excitation with an appreciable yield. Nevertheless, it can be populated by collision and the study of its emission is a theoretical experiment which is very useful for illustrating the conical intersection effects.

As in Ref. [19] we considered a time window from 150 to 300 ns and we computed the photon-counting spectra, $S(\omega)$, (Eq. 5) which are reported in Fig. 2. The result is striking. In fact, because of the nonadiabatic couplings, the maximum of the emission is shifted by more than 9000 cm^{-1}, from 4792 cm^{-1} in the diabatic case (central panel) to 13843 cm^{-1} in the nonadiabatic one. The reason for this is the mixing of the 1^2B_2 (1,0,4) state with the other 1^2B_2 species as (4,3,0), (6,0,0), and (0,10,0), which strongly emit toward the lowest states of the system as can be seen, for example, in the top panel of Fig. 2, where we report $S(\omega)$ of 1^2B_2 (4,3,0). These transitions are strong because of the FC overlaps with the lowest states of the system and because of the ω^3 dependence of the decay rate. It comes out that the ratio between the rates of the fastest decay channel of 1^2B_2 (4,3,0) [toward 1^2A_1 (0,3,0) with a photon of 14826 cm^{-1}] and the fastest decay channel of 1^2B_2 (1,0,4) (toward a 1^2A_1 state too high in energy for assignment, with the emission of a photon of 4792 cm^{-1}) is about 84. Because of this, even small mixing with states which have good FC access to the lowest part of the spectrum greatly modifies the fluorescence of 1^2B_2 (1,0,4). Also the contributions of 1^2B_2 (3,0,2) and (2,2,2), which emit in the same frequency range as 1^2B_2 (1,0,4) because of the excited antisymmetric streching, are important. Indeed, even in this range, the assignments of the levels reached by the emission from the nonadiabatic state do not coincide with those populated from the 1^2B_2 (1,0,4) diabatic state.

[1] (v_1, v_2, v_3), where v_1, v_2 are v_3 are the symmetric stretch, the bending, and the antisymmetric stretch quantum numbers, respectively

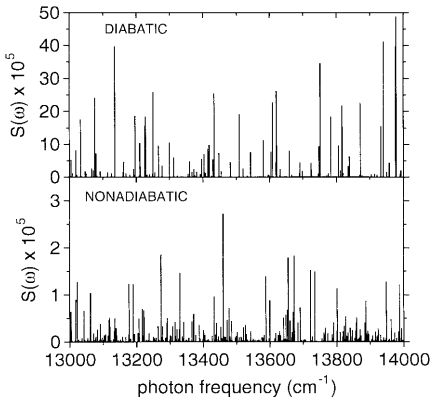

Fig. 3. Time- and frequency-resolved photon-counting spectra of nonstationary states computed in the time window from 150 to 300 ns

4.3 Conical intersection effects on the emission from a nonstationary state

In this section we show the effect of the $\tilde{X}^2A'/\tilde{A}^2A'$ conical intersection on the spontaneous emission from a nonstationary state. Suppose that at time $t = 0$ a rectangular pulse in the frequency domain, from 0 to 18735 cm^{-1}, excites the molecule and let us count the photons emitted in the time window 150–300 ns. The computed spectra in the diabatic case (upper panel) and in the nonadiabatic one (lower panel) are reported in Fig. 3. First note that, as should be expected, the spectra from a nonstationary level contain many more lines than those from stationary levels. Thus, for the sake of clarity, we report the results in a much sharper frequency window with respect to Fig. 2, from 13000 to 14000 cm^{-1}.

The figure shows that the nonadiabatic couplings shift the emitted frequencies owing to the energy shifts of the molecular eigenstates. Furthermore, there is a large redistribution of the emission intensities due to the mixing of the BO states: in the frequency range considered the emission maximum changes from 13979 cm^{-1} in the diabatic case to 13460 cm^{-1} in the nonadiabatic case and the density of the lines grows sensibly in the latter case with respect to the diabatic one. Finally, the diabatic spectrum is more intense than the nonadiabatic one. Indeed, in the time window considered, the shorter the radiative lifetime of the initial state the stronger the emission (Eqs. 2 and 3) and, because of the nonadiabatic mixing of bright and dark states, diabatic lifetimes are, in general, much shorter than the nonadiabatic ones [12].

5 Conclusion

In this article we have analyzed the effect of the $\tilde{X}^2A'/\tilde{A}^2A'$ conical intersection between the first two adiabatic surfaces of NO_2 on the fluorescence of the molecule by computing time- and frequency-resolved spectra for some initial stationary and nonstationary states. We have shown that the conical intersection slows down the fluorescence and sensibly modifies the shapes of the spectra by shifting the emitted frequencies, redistributing the intensities, and increasing the density of the lines. Furthermore, we have shown that the low fluorescence yield observed by Dulcey et al. [19] is due to a considerable emission of photons of energy lower than the investigated range. The spectra of nonstationary states do not reflect the features of the internal dynamics since they are computed at times in which the wave packet has already come to a complete dephasing [11]. We have also worked out a theoretical scheme for computing time- and frequency-resolved spectra at shorter times while the internal dynamics is still developing. It will be the subject of a future work.

Acknowledgements. We thank A. Lami (ICQEM of CNR, Pisa) and C. Petrongolo (Dipartimento di Chimica, Siena) for many useful discussions and suggestions. This work has been supported by the MURST, the CNR, and the ICQEM of Pisa, Italy.

References

1. Köppel H, Domcke W, Cederbaum LS (1984) Adv Chem Phys 57: 59
2. Domcke W, Stock G (1997) Adv Chem Phys 100: 1
3. Ferretti A, Lami A, Villani G (1999) J Chem Phys 111: 916
4. Ionov SI, Davis HF, Mikhaylichenko K, Valachovic L, Beaudet RA, Wittig C (1994) J Chem Phys 1010: 4809
5. Ionov PI, Bezel I, Wittig C (1995) In Chergui M (ed) Femtochemistry. World Scientific, Singapore, p 143
6. Reid SA, Sanov A, Reisler H (1995) Faraday Discuss 102: 129
7. Abel B, Hamann HH, Lange N (1995) Faraday Discuss 102: 147
8. Georges R, Delon A, Jost R (1995) J Chem Phys 103: 1732
9. Reid SA, Reisler H (1996) J Phys Chem 100: 474
10. Brandi R, Santoro F, Petrongolo C (1997) Chem Phys 225: 55
11. Kirmse B, Delon A, Jost R (1998) J Chem Phys 108: 6638
12. Biesheuvel CA, Bulthuis J, Janssen MHM, Stolte S, Snijders JG (1998) J Chem Phys 109: 9701
13. Abel B, Longe N, Reiche F, Troe J (1999) J Chem Phys 110: 1389
14. Abel B, Longe N, Reiche F, Troe J (1999) J Chem Phys 110: 1404
15. Delon A, Jost R (1999) J Chem Phys 110: 4300
16. Santoro F, Petrongolo C (1999) J Chem Phys 110: 4419
17. Mahapatra S, Köppel H, Cederbaum LS (1999) J Chem Phys 110: 5691
18. Santoro F, Petrongolo C (1999) J Chem Phys 111 (in press)
19. Dulcey CS, McGee TJ, McIlarty TJ (1980) Chem Phys Lett 76: 80
20. Santoro F (1999) PhD thesis Universita' di Siena
21. Neuberger D, Duncan ABF (1954) J Chem Phys 22: 1693